

Band offsets of $\text{Al}_2\text{O}_3/\text{In}_x\text{Ga}_{1-x}\text{As}$ ($x=0.53$ and 0.75) and the effects of postdeposition annealing

N. V. Nguyen,^{1,a)} M. Xu,² O. A. Kirillov,¹ P. D. Ye,² C. Wang,^{2,3} K. Cheung,¹ and J. S. Suehle¹

¹Semiconductor Electronics Division, National Institute of Standards and Technology, Gaithersburg, Maryland 20899, USA

²School of Electrical and Computer Engineering and Birck Nanotechnology Center, Purdue University, West Lafayette, Indiana 47907, USA

³Department of Microelectronics, Fudan University, Shanghai 200433, China

(Received 29 September 2009; accepted 11 January 2010; published online 2 February 2010)

Band offsets at the interfaces of $\text{In}_x\text{Ga}_{1-x}\text{As}/\text{Al}_2\text{O}_3/\text{Al}$ where $x=0.53$ and 0.75 were determined by internal photoemission and spectroscopic ellipsometry. The photoemission energy threshold at the $\text{In}_x\text{Ga}_{1-x}\text{As}/\text{Al}_2\text{O}_3$ interface was found to be insensitive to the indium composition but shifted to a lower energy after a postdeposition annealing at high temperatures. Subthreshold electron photoemission was also observed for the annealed sample and was attributed to interfacial layer formation during the annealing process. © 2010 American Institute of Physics.

[doi:10.1063/1.3306732]

High-mobility III-V compound semiconductor channel materials coupled with a high- κ gate dielectric have recently become a major focus as a possible technology to support the further scaling of the advanced complementary metal-oxide-semiconductor (MOS) field-effect transistors technology.¹ While significant progress has been made recently,^{2,3} many challenges remain. One of the main challenges is the formation of a high quality gate dielectric-substrate interface. Many high- κ oxides have been investigated throughout the years including molecular-beam epitaxial $\text{Ga}_2\text{O}_3/\text{Gd}_2\text{O}_3$ mixture,⁴ atomic layer deposited (ALD) Al_2O_3 ,⁵ HfO_2 ,⁶ and $\text{HfO}_2/a\text{Si}$.⁷ The existing consensus is that the native oxide on the III-V compound substrate must be avoided prior to the deposition/growth of the gate oxides. Also at the interface, the oxides must also have band offsets larger than 1 eV to serve as an effective barrier for both electrons and holes to prevent unacceptably large leakage current.⁸ In this letter, combining internal photoemission (IPE) with spectroscopic ellipsometry (SE), we investigated the energy barrier and band offsets at interfaces of ALD Al_2O_3 on $\text{In}_{0.53}\text{Ga}_{0.47}\text{As}$ and $\text{In}_{0.75}\text{Ga}_{0.25}\text{As}$ substrates. The interest in higher indium content composition is due mainly to the higher achievable drive current.⁹ The smaller band gap of the high indium content InGaAs substrate also moves the contact Fermi level closer to the contact metal conduction band leading to a more ideal ohmic contact.¹⁰ The energy barrier height from the top valence band of the InGaAs to the bottom conduction band of Al_2O_3 is found to be essentially the same for both indium concentrations. We also observed a barrier energy lowering phenomenon due to high temperature annealing. It appears that annealing induces the formation of an interfacial layer between the substrate and the oxide.

In this study, MOS structures consisting of Al gate, Al_2O_3 insulator, and both p+ and n+ doped $\text{In}_{0.53}\text{Ga}_{0.47}\text{As}$ and $\text{In}_{0.75}\text{Ga}_{0.25}\text{As}$ were used.¹¹ An 8 nm Al_2O_3 layer was grown by atomic-layer deposition after removing the native surface oxide by a buffered-oxide-etch solution and soaking in ammonium sulfide for 10 min. Postdeposition annealing

(PDA) in N_2 gas was performed at 650 and 600 °C for 30 s. A 12 nm thick Al layer was then thermally evaporated on top of Al_2O_3 . IPE measurements were performed with the bias applied to the substrate from -2 to 2.0 V in steps of 0.1 V, and the photoemission yield is calculated as the ratio of the measured photocurrent to the incident light flux. The electric field in the Al_2O_3 layer was the applied voltage minus the built-in potential which was estimated at the applied voltage when the photocurrent switched direction (see Fig. 1). The dielectric functions of $\text{In}_{0.53}\text{Ga}_{0.47}\text{As}$, $\text{In}_{0.75}\text{Ga}_{0.25}\text{As}$ and Al_2O_3 , and the Al_2O_3 band gap were determined by SE.

The pseudodielectric function of Al_2O_3 is found to be essentially the same for all samples. In Fig. 1 the Al_2O_3 optical band gap of 6.8 eV was determined from the Tauc plot.¹² Figure 2(a) shows the imaginary part (ϵ_2) of the pseudodielectric functions of $\text{In}_{0.75}\text{Ga}_{0.25}\text{As}$ and $\text{In}_{0.53}\text{Ga}_{0.47}\text{As}$ with the three critical points E_1 , $E_1+\Delta_1$, and

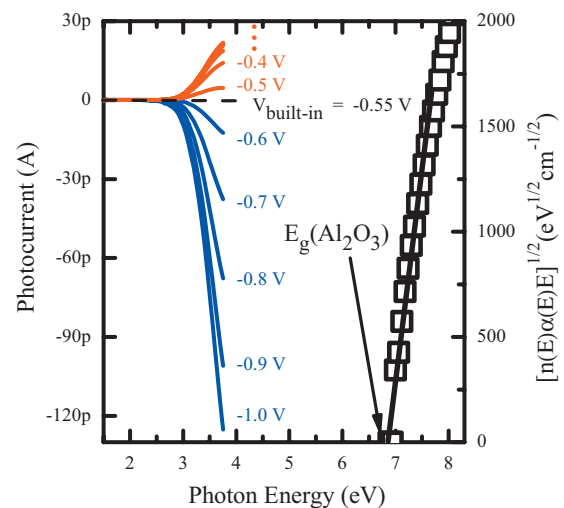


FIG. 1. (Color) Typical photocurrents of PDA $\text{Al}_2\text{O}_3/\text{In}_{0.75}\text{Ga}_{0.25}\text{As}$ sample with the substrate biased from -2 to 0 V to demonstrate how the oxide built-in potential is determined. The current switches direction at about -0.55 V, which is the built-in voltage. The Al_2O_3 band gap is extracted from the Tauc-plot (right axis) by linear fitting of $[n(E)\alpha(E)]^{1/2}$ where $n(e)$ is the index of refraction and $\alpha(E)$ the absorption coefficient.

^{a)}Author to whom correspondence should be addressed. Electronic mail: nhan.nguyen@nist.gov.

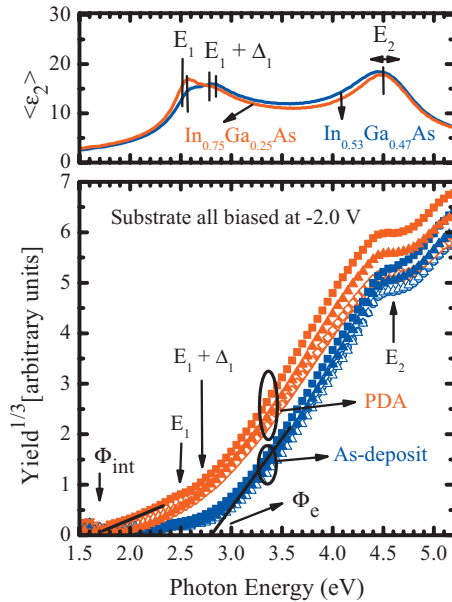


FIG. 2. (Color) Imaginary part (ϵ_2) of the pseudodielectric function of $\text{In}_{0.53}\text{Ga}_{0.47}\text{As}$ (blue curve) and $\text{In}_{0.75}\text{Ga}_{0.25}\text{As}$ (red curve). Red-colored and blue-colored symbols (bottom graph) are cube root of the IPE yield as a function of photon energy for PDA and as-deposited Al_2O_3 , respectively. Filled and open symbols correspond to n-type and p-type substrate, respectively. All the IPE data shown were taken with the substrate biased at -2.0 V.

E_2 which are shifted to lower energy for higher indium concentration.¹³ Reductions in the photocurrent are seen between 2.4 and 2.8 eV and between 4.5 and 4.8 eV [Fig. 2(b)]. The reduction at E_2 is due to the strong absorption or the decreasing light penetration depth and the X_5 critical point final state of the E_2 transition in the X crystal momentum direction being well below the Al_2O_3 bottom conduction band.¹⁴

A series of $Y^{1/3}-h\nu$ plots, shown in Fig. 2(b), measured at a substrate bias of -2.0 V for all samples, clearly indicate that PDA samples have a lower energy threshold than those of as-deposited samples. The spectral thresholds (Φ_e 's) extracted by linear fits correspond to IPE from the InGaAs valence band maximum to the Al_2O_3 conduction band minimum. A 0.3 eV redshift is observed for all annealed samples with respect to the as-deposited samples. A similar redshift was reported when GaAs surface was treated,¹⁵ leading us to speculate that, the shift may be caused by the interfacial chemical modification. It also is interesting to note that when Al_2O_3 is annealed at much higher temperature (>800 °C), a blueshift was observed and attributed to the Al_2O_3 phase change.¹⁶

Another significant observation is the subthreshold IPE signals as indicated by Φ_{int} in Fig. 2(b), possibly due to the formation of an interlayer between the substrate and Al_2O_3 . Similar subthreshold photoemission has been shown to originate from an intentionally grown interlayer between the III-V substrates and the Al_2O_3 and HfO_2 gates.¹⁷ While we have no direct evidence, this layer is likely to be a mixture of oxides or suboxides containing Ga, As, and In where In oxide does not seem to play a significant role to the band offset as discussed below. Furthermore, the high temperature PDA induced a thicker interfacial layer with a higher state density as evidenced by a stronger emission below the principal threshold (Φ_e). For the as-deposited samples, a weaker sub-

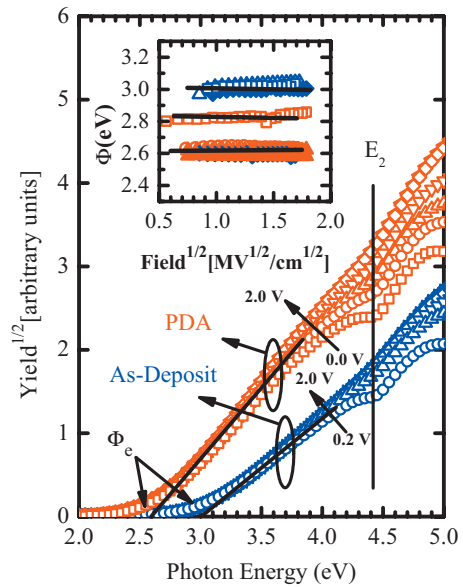


FIG. 3. (Color) Typical Powell plots of Al/p -type $\text{In}_{0.53}\text{Ga}_{0.47}\text{As}$ for PDA samples (red) and as-deposited (blue) measured at substrate bias from 0.0 or 0.2 V to $+2.0$ V. The inset Schottky plots show field dependence of the barrier heights for all PDA (red) and as-annealed (blue) samples; open and closed symbols correspond to p-type and n-type substrates, respectively.

threshold signal [see Fig. 2(b)] is indicative of a thinner interfacial layer. The same conclusion is suggested by the relatively weaker E_1 and $E_1 + \Delta_1$ features in the IPE signal.

The spectral thresholds (Φ_e) were determined by fitting the conventional Fowler plots $Y^{1/2}-h\nu$ as shown in Fig. 3. The subthreshold tails are believed to relate to the conduction band tail states of Al_2O_3 and/or the lateral nonuniformity of the barrier.¹⁸ Schottky plots depicted in the inset of Fig. 3 display a rather weak field dependence of the $\text{Al}/\text{Al}_2\text{O}_3$ barrier heights for all samples as indicated by three different values in the inset figure. The barrier height variation does not have a consistent relation with the treatment condition of Al_2O_3 . Since the Al_2O_3 surface was exposed to air ambient for a long period of time prior to Al deposition, it is quite probable that the contamination may contribute to the variation, as it is well known that the $\text{Al}/\text{Al}_2\text{O}_3$ electronic interface properties are strongly dependent on growth and surface conditions. In fact, metal/high- κ oxide interface barriers have been shown a strong sensitivity to the interface chemical nature.¹⁹ It is also noticed that, since the IPE quantum yields are much weaker for the large barrier height samples, it is indicative of lower interfacial transition probabilities of photocarriers accumulated at the larger barrier height interface. Furthermore, external field dependence of the barrier height is almost constant; i.e., very insensitive to the applied external electric field. In contrast to the metal/ SiO_2 systems where the image-force interaction is significant, it has been documented that such interaction is much reduced in the metal/high- κ system. It has been suggested that the cause of barrier height insensitivity is likely due to the existence of a plane of negative charges distributed in the high- κ close to the metal.¹⁸

Figure 4 displays a series of Schottky plots characterizing the Al_2O_3 electric field dependence of the barrier heights (Φ_e) at the $\text{Al}_2\text{O}_3/\text{InGaAs}$ interface for all samples. Within 0.1 eV uncertainties, the zero-field barrier heights (Φ_e^0) of as-deposit and PDA Al_2O_3 on $\text{In}_{0.53}\text{Ga}_{0.47}\text{As}$ and

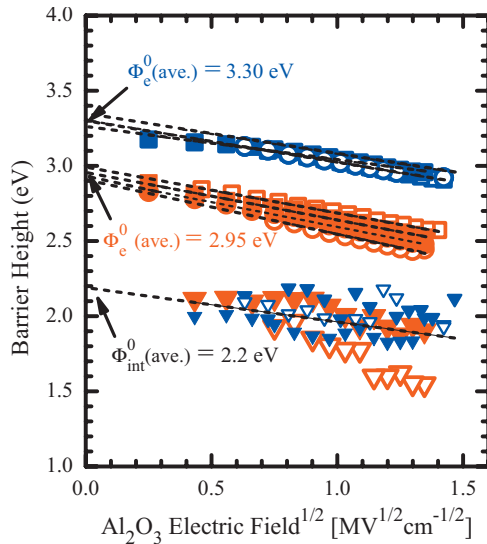


FIG. 4. (Color) Schottky plots for oxide field dependence of the barrier heights at the $\text{Al}_2\text{O}_3/\text{InGaAs}$ interface for all samples: blue color for as-deposited Al_2O_3 , red color for PDA Al_2O_3 , open symbols for p-type substrates, and filled symbols for n-type substrates. Φ_e^0 and Φ_{int}^0 are the averaged zero-field barrier heights at $\text{Al}_2\text{O}_3/\text{InGaAs}$ and for the interlayer, respectively.

$\text{In}_{0.75}\text{Ga}_{0.25}\text{As}$ substrates can be reasonably averaged to a value of 3.30 and 2.95 eV, respectively. Therefore it is concluded that the effect of PDA is to reduce the barrier height of 0.35 eV which is also clearly seen as a redshift in Fig. 1. The barrier height value from *as-deposited* Al_2O_3 is in good agreement with the reports of the IPE study on *unannealed* ALD Al_2O_3 on $\text{In}_{1-x}\text{Ga}_x\text{As}_x$ where the indium varied from 0% to 53%.²⁰ It is also illuminating to compare our results with the recent X-ray photoelectron spectroscopy and reflection electron energy loss spectroscopy study²¹ where the authors showed that the barrier height of 600 °C -annealed ALD on $\text{In}_{1-x}\text{Ga}_x\text{As}_x$ ($x < 0.5$) varied from 2.84 to 3.11 eV, which is consistent with the lower barrier height obtained from PDA samples in this study. It is important to note that within the measurement uncertainty the barrier height does not change with respect to the large indium concentration difference. This means that the top of the valence band pins at the same energy position with respect to the bottom Al_2O_3 conduction band. The same conclusion was reached by a similar study but with the lower indium concentration (<50%) in the In-GaAs (Ref. 20) and theoretically predicted⁸ where they show a much larger offset of the conduction band than that of valence band for GaAs and InAs.

From the band gaps of $\text{In}_{0.53}\text{Ga}_{0.47}\text{As}$ and $\text{In}_{0.75}\text{Ga}_{0.25}\text{As}$ being 0.75 and 0.55 eV, respectively, we conclude that the conduction band offset is 2.55 and 2.75 eV for as deposited Al_2O_3 on $\text{In}_{0.53}\text{Ga}_{0.47}\text{As}$ and $\text{In}_{0.75}\text{Ga}_{0.25}\text{As}$, respectively, and 2.20 and 2.40 eV for PDA Al_2O_3 on $\text{In}_{0.53}\text{Ga}_{0.47}\text{As}$ and $\text{In}_{0.75}\text{Ga}_{0.25}\text{As}$, respectively. However, the valence band offset is essentially the same for both substrates since the barrier heights were found insensitive to the indium content. Therefore, from the Al_2O_3 band gap of 6.80 eV measured by SE, the valence band offset becomes 3.85 and 3.50 eV for PDA and as-deposited Al_2O_3 , respectively. Figure 4 also displays that the zero-field barrier height of the interlayer was averaged to a value of 2.2 ± 0.3 eV. The annealing effect and the existence of the interlayer appear to degrade the current-

voltage characteristics as we find that ALD Al_2O_3 have higher leakage currents than that of as-deposited samples (not shown). Finally, with the conduction band offset much larger than 1.0 eV,⁸ ALD Al_2O_3 should be suitable to use in a high mobility MOS device as long as the formation of the interlayer of lower barriers can be avoided, and the substrate surface chemistry must be well controlled to achieve stable and reliable devices.²²

In summary, using internal photoemission and SE we study the band offsets of atomic-layer-deposited Al_2O_3 on two different indium concentration substrates, $\text{In}_{0.53}\text{Ga}_{0.47}\text{As}$ and $\text{In}_{0.75}\text{Ga}_{0.25}\text{As}$, and subjected then to postdeposition annealing. The barrier height is found to be insensitive to the indium amount. When comparing as-deposited and postdeposition annealed Al_2O_3 , we find a redshift to 0.3 eV of the barrier height when Al_2O_3 is annealed at high temperature. In addition, a spectral subthreshold was clearly observed in annealed Al_2O_3 , implying the formation of an interlayer of possible different chemical nature under thermal annealing.

Three of the authors (N.V.N., C.K., and J.S.S.) gratefully acknowledge funding from the NIST Office of Microelectronics Programs and Intel Corporation.

¹P. D. Ye, *IEEE Spectrum* **45**, 42 (2008).

²R. J. W. Hill, D. A. J. Moran, X. Li, H. Zhou, D. Macintyre, S. Thoms, A. Asenov, P. Zurcher, K. Rajagopalan, J. Abrokwah, R. Droopad, M. Passlack, and L. G. Thyne, *IEEE Electron Device Lett.* **28**, 1080 (2007).

³Y. Xuan, Y. Q. Wu, and P. D. Ye, *IEEE Electron Device Lett.* **29**, 294 (2008).

⁴M. Passlack, M. Hong, J. P. Mannaerts, R. L. Opila, S. N. G. Chu, N. Moriya, F. Ren, and J. R. Kwo, *IEEE Trans. Electron Devices* **44**, 214 (1997).

⁵Y. Xuan, Y. Q. Wu, H. C. Lin, T. Shen, and P. D. Ye, *IEEE Electron Device Lett.* **28**, 935 (2007).

⁶K. Y. Lee, Y. J. Lee, P. Chang, M. L. Huang, Y. C. Chang, M. Hong, and J. Kwo, *Appl. Phys. Lett.* **92**, 252908 (2008).

⁷S. Koveshnikov, W. Tsai, I. Ok, J. C. Lee, V. Torokanov, M. Yakimov, and S. Oktyabrsky, *Appl. Phys. Lett.* **88**, 022106 (2006).

⁸J. Robertson and B. Falabretti, *J. Appl. Phys.* **100**, 014111 (2006).

⁹K. Kalna, R. Droopad, M. Passlack, and A. Asenov, *Microelectron. Eng.* **84**, 2150 (2007).

¹⁰T. C. Shen, G. B. Gao, and H. Morkoc, *J. Vac. Sci. Technol. B* **10**, 2113 (1992).

¹¹Y. Xuan, P. D. Ye, and T. Shen, *Appl. Phys. Lett.* **91**, 232107 (2007).

¹²N. V. Nguyen, S. Sayan, I. Levin, J. R. Ehrstein, I. J. R. Baumvol, C. Driemeier, C. Krug, L. Wielunski, P. Y. Hung, and A. Diebold, *J. Vac. Sci. Technol. A* **23**, 1706 (2005).

¹³T. J. Kim, T. H. Ghong, Y. D. Kim, S. J. Kim, D. E. Aspnes, T. Mori, T. Yao, and B. H. Koo, *Phys. Rev. B* **68**, 115323 (2003).

¹⁴J. R. Chelikowsky and M. L. Cohen, *Phys. Rev. B* **14**, 556 (1976).

¹⁵N. V. Nguyen, O. A. Kirillov, W. Jiang, W. Wang, J. S. Suehle, P. D. Ye, Y. Xuan, N. Goel, K. W. Choi, W. Tsai, and S. Sayan, *Appl. Phys. Lett.* **93**, 082105 (2008).

¹⁶V. V. Afanas'ev, A. Stesmans, B. J. Mrstik, and C. Zhao, *Appl. Phys. Lett.* **81**, 1678 (2002).

¹⁷V. V. Afanas'ev, M. Badylevich, A. Stesmans, G. Brammertz, A. Delabie, S. Sionke, A. O'Mahony, I. M. Povey, M. E. Pemble, E. O'Connor, P. K. Hurley, and S. B. Newcomb, *Appl. Phys. Lett.* **93**, 212104 (2008).

¹⁸V. V. Afanas'ev, *Internal Photoemission Spectroscopy: Principles and Applications* (Elsevier, Amsterdam, 2008).

¹⁹V. V. Afanas'ev and A. Stesmans, *J. Appl. Phys.* **102**, 081301 (2007).

²⁰V. V. Afanas'ev, A. Stesmans, G. Brammertz, A. Delabie, S. Sionke, A. O'Mahony, I. M. Povey, M. E. Pemble, E. O'Connor, P. K. Hurley, and S. B. Newcomb, *Appl. Phys. Lett.* **94**, 202110 (2009).

²¹M. L. Huang, Y. C. Chang, Y. H. Chang, T. D. Lin, J. Kwo, and M. Hong, *Appl. Phys. Lett.* **94**, 052106 (2009).

²²C. L. Hinkle, M. Milojevic, E. M. Vogel, and R. M. Wallace, *Microelectron. Eng.* **86**, 1544 (2009).